

## LOAD POSITIONING AND MINIMIZATION OF LOAD OSCILLATIONS IN ROTARY CRANES

ANDRZEJ MACZYŃSKI

*Department of Mechanics and Computer Methods, University of Bielsko-Biala  
e-mail: amaczyński@ath.bielsko.pl*

In the paper a method of load positioning and minimization of load final oscillations in rotary cranes has been presented. Drive functions of the slewing of an upper structure have been determined by means of dynamic optimisation. In the optimisation task a simplified model has been used. A completely stiff supporting structure of the crane has been assumed. A feedback control system has been proposed to compensate for influences of flexibilities that have not been taken into account during the optimisation and for inaccurate knowledge of parameters of the model. The effectiveness of the control system for two different controlled variables has been analysed. A special coefficient for quantitative analysis has been proposed. Results of numerical simulations have been presented.

*Key words:* crane, positioning, control, numerical simulation

### 1. Introduction

The limitation of load oscillations during the slewing motion of a crane upper structure and, especially, during the final load positioning is a vital problem for the effectiveness and occupational safety of the reloading and assembly work. This explains why the problem of minimization of load oscillations in rotary cranes is taken up in many papers (Abdel-Rahman and Nayfeh, 2002; Balachandran *et al.*, 1999; Bednarski *et al.*, 1997; Kłosiński, 2000; Parker *et al.*, 1995; Sakawa *et al.*, 1981). Mobile cranes belong to the kind of cranes for which accident hazard is extreme (Neitzel *et al.*, 2001; Yow *et al.*, 2000). That is why the author has been carrying out research connected with load positioning at the end of the slewing motion of a mobile telescopic crane for

several years. One of the most important assumptions in author's investigations is that it is possible to determine the drive functions which minimize the final load oscillations by using optimisation methods and a simplified model. In this simplified model, a completely stiff supporting structure of the crane may be assumed. The influence of flexibilities that are not taken into account during the optimisation, and inaccurate knowledge of parameters of the model can be compensated by a feedback control system with a PID controller. The appropriate choice of a controlled variable is fundamental for the operation efficiency of the control system. This variable should also be easily measured. Comparison of the control system effectiveness for two different controlled variables is presented in the paper.

## 2. Determination of functions of the upper structure slewing. The dynamic model of a crane

Drive functions of the upper structure slewing have been determined from the point of view of minimization of final load oscillations and, simultaneously, load positioning (Maczyński and Wojciech, 2000). In this task a simplified model, taking into account the complete stiffness of the crane supporting structure, has been used. The Nelder-Meads method has been applied. The objective function is defined as follows

$$F = C_1 \frac{1}{2} m_L v_{LT}^2 + C_2 \| \mathbf{r}_{LT} - \mathbf{r}_{LF} \|^2 \quad (2.1)$$

where

$$\mathbf{r}_{LT} = \mathbf{r}_L \Big|_{t=T} \quad v_{LT} = v_L \Big|_{t=T}$$

and

- $m_L$  – mass of the load
- $\mathbf{r}_{LF}$  – vector of expected load coordinates at the moment  $t = T$
- $\mathbf{r}_L$  – vector of load coordinates
- $v_L$  – velocity of the load
- $T$  – time of the upper structure's slewing
- $C_1, C_2$  – coefficients (weights).

This objective function means that one can expect that at the end of the slewing motion the load is at a particular point in space and, furthermore, its kinetic energy is minimal. Values of the coefficients  $C_1$  and  $C_2$  have been

determined during numerical simulations. The main criterion of this determination was the best quality of load positioning at the end of the slewing motion.

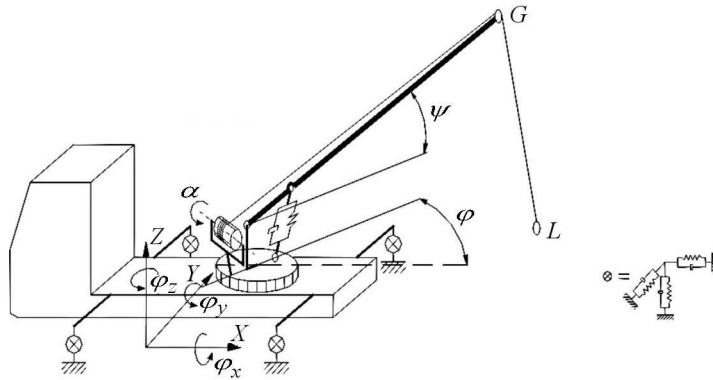


Fig. 1. Flexible model of a mobile crane

Figure 1 shows the model of a crane that has been used to perform numerical simulations presented below. It is a 3D model which takes into account the flexibility of the crane supporting structure and damping in selected subsystems. It allows dynamic analysis of a telescopic mobile crane in every respect, and is described in detail in Maczyński and Szczotka (2002).

### 3. The feedback control system – determination of controlled variables

In this section the feedback control system, which compensates for the influence of the flexibilities ignored during the optimisation of load positioning, is briefly discussed. The control system can also eliminate the influence of inaccurate knowledge of parameters of the model.

Figure 2 presents a block diagram of the control system. It is a programmed control system. Functions of the controlled variable  $\Phi_t$  have been calculated for the simplified model, the optimal drive function and for certain operating parameters. The analysis has been carried out for two different controlled variables  $\Phi_t$ :

- angle  $\varphi_L$  of deflection of the load
- angle  $\tau$  of tangential deflection of the load.

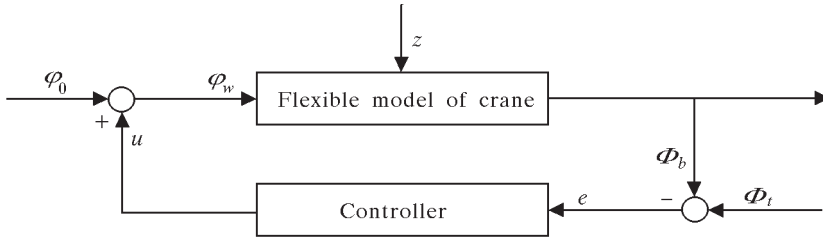


Fig. 2. Block diagram of the control system;  $\varphi_0$  – slewing angle of the crane determined according to Maczyński and Wojciech (2000) (optimal for the simplified model),  $\Phi_t$  – controlled variable determined for the simplified model,  $\Phi_b$  – actual value of the controlled variable

### 3.1. Angle $\varphi_L$ of deflection of the load as the controlled variable

The definition of the angle  $\varphi_L$  of deflection of the load is presented in Fig. 3. The plane marked out by the coordinate system  $0'X'Y'$  is parallel to the ground. The origin of the coordinate system lies on the axis of rotation of the crane upper structure, the axis  $0'X'$  is parallel to the axis  $X$  in Fig. 1. Points  $G'$  and  $L'$  define the projections of the end of the jib and the load on the plane  $X'Y'$ , respectively.

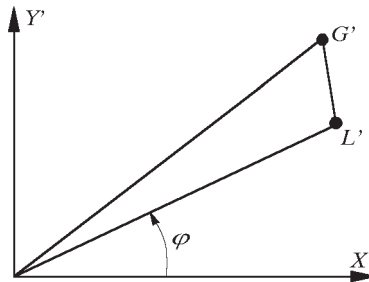


Fig. 3. Angle  $\varphi_L$  of deflection of the load

Author's earlier research demonstrates that assuming the angle  $\varphi_L$  as the controlled variable can give satisfactory results of numerical analysis. The time course of the angle  $\varphi_L$  corresponds well with load oscillations, especially tangential ones, and enables them to be effectively eliminated. However, measurement of the angle  $\varphi_L$  in a real crane is inconvenient and requires the use of expensive measuring devices, for instance laser devices. This solution

would mean a significant increase in the price of the crane, especially in the case of small simple versions. Therefore, another parameter that could be used as the controlled variable has been sought; it is assumed that the angle  $\tau$  of tangential deflection of the load can be treated as the controlled variable.

### 3.2. Angle $\tau$ of tangential deflection of the load as the controlled variable

The diagram in Fig. 4 shows the end of the jib (point  $G$ ) and the load  $L$  that are linked by the rope ( $GL$ ). The angles  $\tau$  of tangential and  $\beta$  of radial deflection of the rope are marked in the figure.

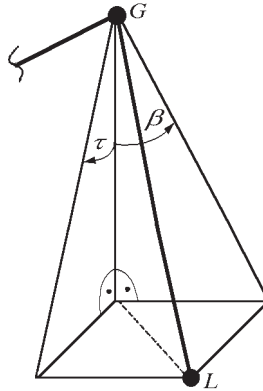


Fig. 4. Angle  $\tau$  of tangential deflection of the load

## 4. Numerical calculations

Masses and geometrical parameters of the model have been chosen for numerical calculations based upon the technical documentation of the DUT 0203 crane. The mass of the load was equal to 3000 kg, the crane radius about 8.7 m. The control system efficiency in compensating the influence of the flexibilities of the crane supporting structure has been analysed for both controlled variables for the following cases of motion:

- slewing by  $60^\circ$  over a period of 12 s
- slewing by  $75^\circ$  over a period of 13.5 s
- slewing by  $90^\circ$  over a period of 15 s.

In graphs presented in this paper, PID\_I denotes courses obtained for the control system with the angle  $\varphi_L$  as the controlled variable, PID\_II – with the angle  $\tau$ . The selection of controller settings has been carried out using the criterion of minimizing load oscillations based on the positioning efficiency coefficient

$$P_{EG} = \sqrt{x_0^2 + y_0^2} \quad (4.1)$$

where

$$x_0 = |x_L - x'_{LF}|_{\max} \quad y_0 = |y_L - y'_{LF}|_{\max}$$

and

- $x_L, y_L$  – coordinates of the load
- $x'_{LF}, y'_{LF}$  – expected load coordinates for  $t = T$
- $|x_L - x'_{LF}|_{\max}, |y_L - y'_{LF}|_{\max}$  – maximal absolute value of the difference between the coordinates after the end of the slewing motion.

The load coordinates  $x'_{LF}, y'_{LF}$  expected at the time  $t = T$  have been determined for the static load of the crane for a given final angle of the slewing and mass of the load. During calculation of the coefficient value, it is important that the time of load observation after the end of the crane slewing must be longer than the time of load oscillations.

Numerical simulations showed that good quality of load positioning, for all three analysed motions, can be obtained using the controller type  $P$ . Application of integrating and/or differential elements of the controller did not cause significant improvement of the positioning efficiency. In the analyses it has been assumed that the proportional gain  $K_c$  was equal to 20 for PID\_I and 0.95 for PID\_II.

Figure 5 shows the final parts of the load trajectories for motions 1-3, respectively. In graphs, besides curves denoted by PID\_I and PID\_II, the curve obtained for the drive without the feedback control system is also presented. Additionally, point ■ is the theoretical point at which the load should stop at the end of the slewing motion. This theoretical point has been determined for the static load and for the model taking into consideration the flexibilities of the crane supporting structure.

In Table 1 values of the  $P_{EG}$  coefficient for the analysed cases are compared.

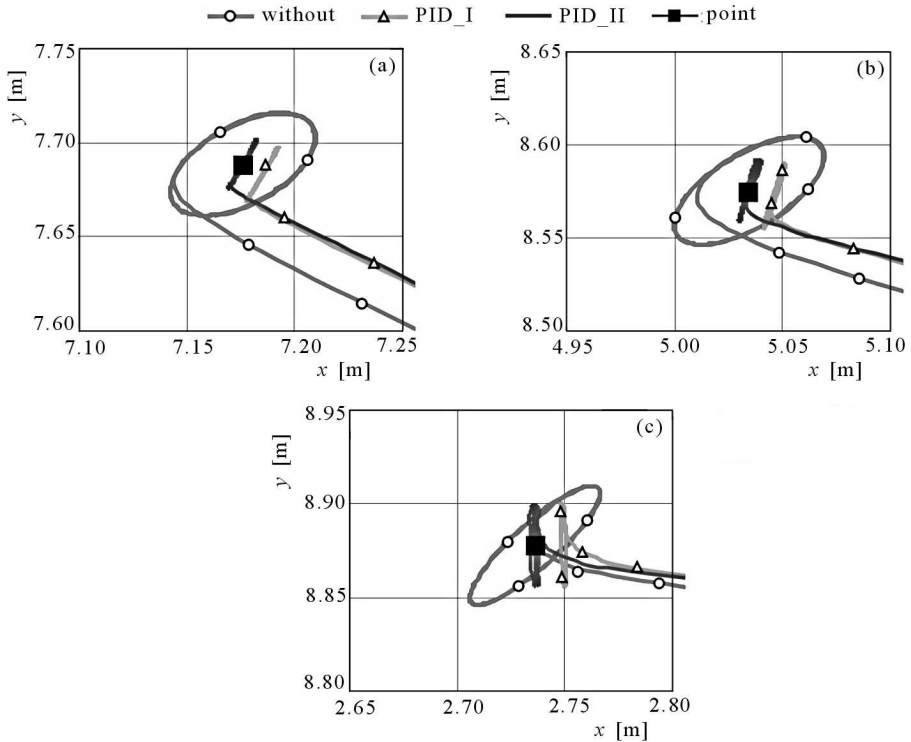


Fig. 5. Slewing by 60° (a), 75° (b) and 90° (c)

**Table 1.** Comparison of  $P_{EG}$  coefficient values

Angle	$P_{EG}$ coefficient value [cm]		
	without control system	PID_I	PID_II
60°	4.37	2.57	1.56
75°	4.59	2.71	1.81
90°	4.42	2.70	2.21

The data in Table 1 show considerable differences between the values obtained for the control system PID\_I and PID\_II. According to the case of the slewing analysed, the differences range from 22% to 65%. The assessment of the final load positioning carried out by means of observation of the load trajectories does not confirm these differences (Fig. 5). The quality assessment in fact shows that the final load oscillations are more or less equal for both feedback control systems. However, a certain displacement between the load

trajectories after the end of the crane slewing can be seen. This displacement causes differences in values of the coefficient  $P_{EG}$ , as shown in Table 1.

The  $P_{EG}$  coefficient was defined for the drive without the feedback control system. In this type of drive, the expected load position after the end of the motion is identical to the load position in static conditions. However, in the case of the drive with the feedback control system, the expected load position depends on the controlled variables. The angle  $\varphi_L$  contains information about the load position in static conditions. When determining the desired value of the angle  $\varphi_L$ , the simplified model omitting the flexibilities of the crane structure is used. Thus, the feedback control system tries to change the final load position and to place the load as in the simplified model. However, the angle  $\tau$  contains information only about the relative position of the load and the end of the jib. In this case, the expected load position after the end of the motion is in agreement with the state of equilibrium for the model taking into account the flexibilities. The graph in Fig. 6 confirms this hypothesis. Figure 6 shows the upper structure slewing by  $90^\circ$ . In addition to curves from Fig. 5c, the projection of the load trajectory for the drive without the control system obtained for the simplified model is presented. It is denoted as "simp".

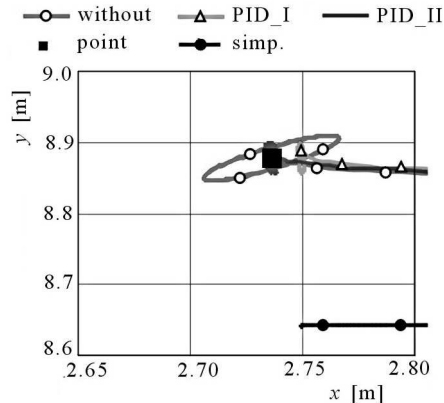


Fig. 6. Comparison of load trajectories for slewing by  $90^\circ$

The differences occurring between the values of the positioning efficiency coefficient  $P_{EG}$  led the author to define the coefficient once again. This new coefficient is denoted as  $P_E$

$$P_E = \sqrt{\left(\frac{x_{\max} - x_{\min}}{2}\right)^2 + \left(\frac{y_{\max} - y_{\min}}{2}\right)^2} \quad (4.2)$$



where  $x_{\max}$ ,  $x_{\min}$ ,  $y_{\max}$ ,  $y_{\min}$  – maximal and minimal values of the load coordinates registered after the end of the slewing of the upper structure, Fig. 7.

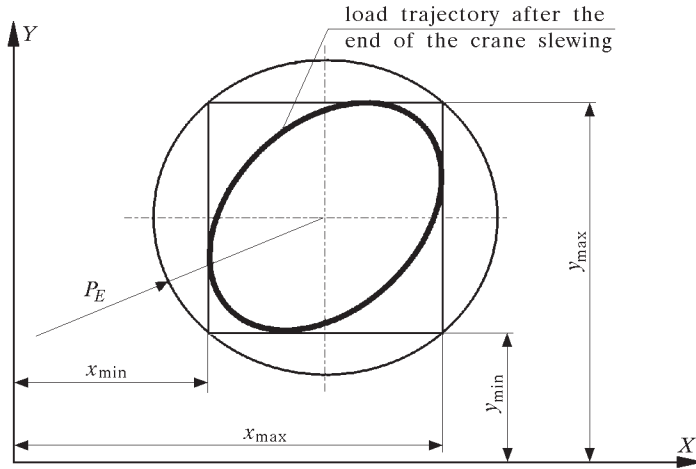


Fig. 7. Geometrical interpretation of the  $P_E$  coefficient

A geometrical interpretation of the  $P_E$  coefficient is presented in Fig. 7. It is the radius of the circle circumscribed onto the rectangle in which the load trajectory (after the end of slewing) is inscribed. Values of the  $P_E$  coefficient calculated for described motions are compared in Table 2.

**Table 2.** Comparison of  $P_E$  coefficient values

Angle	$P_E$ coefficient value [cm]	
	PID_I	PID_II
60°	1.64	1.51
75°	1.86	1.76
90°	2.25	2.19

Results presented in Table 2 show that the  $P_E$  coefficient lacks the  $P_{EG}$  coefficient error. It is in agreement with the quality assessment performed by means of observing the load trajectories.

Figure 8 presents dependencies of the  $P_E$  coefficient values on the proportional gain  $K_c$ . The curves have been obtained for cases of motion 1-3. Graphs in Fig. 8a and Fig. 8b relate to the PID\_I control system (in Fig. 8b the proportional gain  $K_c$  is held within the range  $0 \div 5$ ), Fig. 8c relates to the PID\_II control system.

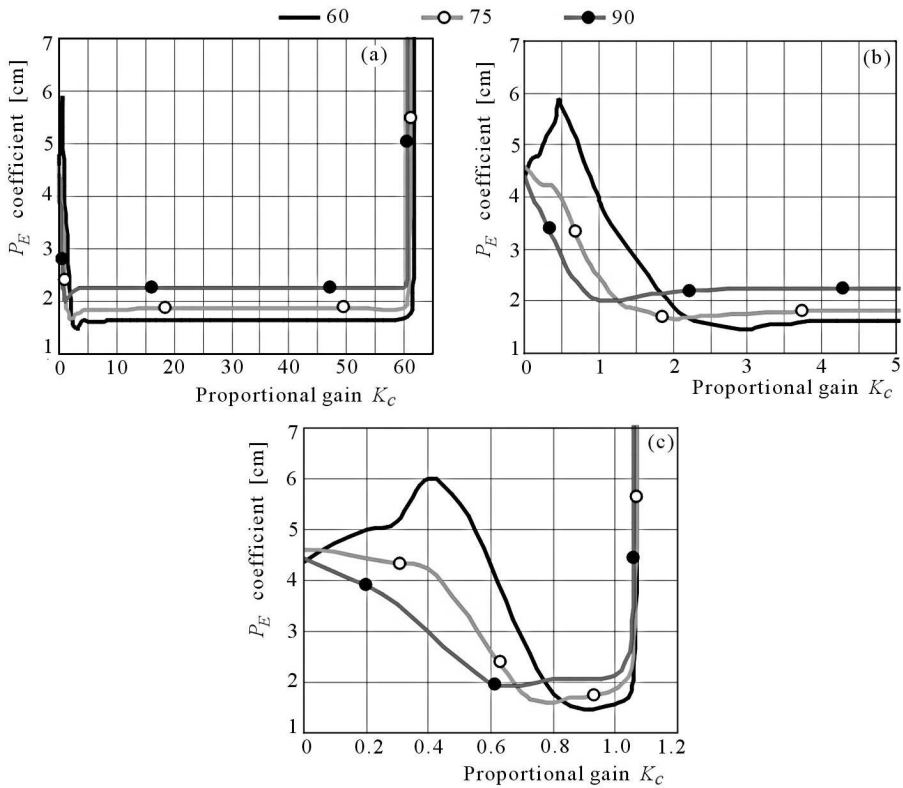


Fig. 8.  $P_E$  coefficient versus proportional gain  $K_c$ ; (a) – PID\_I, (b) – PID\_I and  $K_c = 0 \div 5$ , (c) – PID\_II

Graphs in Fig. 8 show that the control system with the angle  $\varphi_L$  (PID\_I) as the controlled variable is less sensitive to the selection of the proportional gain  $K_c$ . For the proportional gain  $K_c$  in the range  $5 \div 50$  and for all three analysed motions, the  $P_E$  coefficient maintains an almost constant value. This value is only slightly greater than the minimal value of the  $P_E$  coefficient. The minimal values of the  $P_E$  coefficient are obtained for lower values of the proportional gain  $K_c$ . The proportional gain  $K_c$  that ensures the minimum of the  $P_E$  coefficient is different for every slewing. Thus, it is impossible to obtain the minimal value of the  $P_E$  coefficient for one value of the proportional gain  $K_c$  and for all cases of motion. When the value of the proportional gain  $K_c$  exceeds 60, then sudden deterioration in the positioning quality occurs. In the case of the control system with the  $\tau$  angle (PID\_II) as the controlled varia-

ble, the most advantageous values of the  $P_E$  coefficient are obtained for the following ranges of the proportional gain  $K_c$ : motion 1 –  $\langle 0.8, 1.05 \rangle$ , motion 2 –  $\langle 0.7, 1 \rangle$  and motion 3 –  $\langle 0.6, 1 \rangle$ . For the PID\_II, sudden deterioration in the positioning quality occurs when the proportional gain  $K_c$  exceeds 1.05.

## 5. Summary

Numerical simulations prove that the feedback control system presented in the paper effectively compensates for the influence of the flexibility of the crane supporting structure on the final load positioning. Its effectiveness does not depend on the choice of the controlled variable. Results obtained for both angles:  $\varphi_L$  of deflection of the load, and  $\tau$  of tangential deflection, are comparable. The feedback control system minimizes the load oscillations in the tangential direction very effectively but it leaves some in the radial direction. It is impossible to completely eliminate the load oscillations in two directions using for this purpose only one drive motion – the slewing motion of the upper structure. In his future research, the author plans to elaborate a conception of a simple supplementary system that should eliminate the remaining radial oscillations.

From the practical point of view, it is important that taking the  $\tau$  angle as the controlled variable has effects similar to those obtained for the angle  $\varphi_L$ . The only real difference between the results obtained is the small displacement discussed in Section 4. The value of the displacement does not exceed 2 cm, so it is a negligible variable for an operator. The operator is mainly interested in elimination of the final load oscillations. Fig. 8 shows that the PID\_I system is more convenient in terms of the controller setting selection; it enables the positioning quality to be improved over a wide range of values of the proportional gain  $K_c$ . For the PID\_II, this range is much narrower and, even if exceeded only slightly, can cause clear deterioration of the load positioning quality.

The analysis of the results shows that the positioning efficiency coefficient  $P_{EG}$ , used so far by the author, can, in the case of the drive with the feedback control system, be misleading. That is why the new universal coefficient  $P_E$  has been proposed. This new coefficient can be useful during the assessment of the load positioning for drives with or without the control system and any controlled variable. On the basis of the graphs showing dependence of the  $P_E$  coefficient on the  $K_c$  proportional gain (Fig. 8), it is easy to determine the most advantageous settings of the controller. Simulations indicate that a

considerable improvement in the quality of the load positioning is possible for a wide range of drives, using only one value of the controller settings.

The proposed method of the load positioning and oscillation minimization, which has been discussed using the example of a telescopic mobile crane, can be also utilised in the case of other rotary cranes.

## References

1. ABDEL-RAHMAN E.M., NAYFEH A.H., 2002, Pendulation reduction in boom cranes using cable length manipulation, *Nonlinear Dynamics*, **27**, 3, 255-269
2. BALACHANDRAN B., LI Y.-Y., FANG C.-C., 1999, A mechanical filter concept for control of non-linear crane-load oscillations, *Journal of Sound and Vibration*, **228**, 3, 651-682
3. BEDNARSKI S., CINK J., TOMCZYK J., 1997, Pozycjonowanie ładunku w ruchu roboczym żurawia portowego, *Proc. X Konferencji Problemy Rozwoju Maszyn Roboczych*, part I, 25-31
4. KŁOSIŃSKI J., 2000, Slewing motion control in mobile crane ensuring stable positioning of carried load, *The Archive of Mechanical Engineering*, **XLVII**, 119-138
5. MACZYŃSKI A., SZCZOTKA M., 2002, Comparison of models for dynamic analysis of a mobile telescopic crane, *Journal of Theoretical and Applied Mechanics*, **40**, 4, 1051- 1074
6. MACZYŃSKI A., WOJCIECH S., 2000, Selection of function describing crane slewing motion in order to minimize load oscillations, *Proc. XII Conference on "Drives, Control and Automation of Working Machines and Vehicles"*, 317-326 (in Polish)
7. NEITZEL R.L., SEIXAS N.S., REN K.K., 2001, A review of crane safety in the construction industry, *Applied Occupational and Environmental Hygiene*, **16**, 12, 1106-1117
8. PARKER G.G., PETERSON B., DOHRMANN C., ROBINETT R.D., 1995, Command shaping for residual vibration free crane maneuvers, *Proc. American Control Conference*, Seattle, Washington, 934-938
9. SAKAWA Y., SHINDO Y., HASHIMOTO Y., 1981, Optimal control of a rotary crane, *Journal of Optimization Theory and Applications*, **35**, 535-557
10. YOW P., ROTH R., FRY K., 2000, Crane accidents 1997-1999: a report of the crane unit of the division of occupational safety and health, Division of Occupational Safety and Health, California Department of Industrial Relations

## Pozycjonowanie i minimalizacja wahań ładunku w żurawiach obrotowych

### Streszczenie

W pracy zaprezentowano metodę pozycjonowania i minimalizacji końcowych wahań ładunku w żurawiach obrotowych. Funkcja napędowa obrotu nadwozia została dobrana na drodze optymalizacji dynamicznej dla uproszczonego modelu zakładającego całkowitą sztywność układu nośnego żurawia. Zaproponowano układ regulacji kompensujący wpływ nieuwzględnionych podczas optymalizacji podatności i niedokładnej znajomości parametrów modelu. Analizowano działanie układu regulacji dla dwóch różnych wielkości zadanych. Do ilościowej oceny jakości pozycjonowania zaproponowano specjalny wskaźnik. Zaprezentowano wyniki symulacji numerycznych.

*Manuscript received May 5, 2003; accepted for print June 16, 2003*